IOP Publishing Journal of Physics: Condensed Matter

J. Phys.: Condens. Matter **23** (2011) 296003 (8pp) doi:10.1088/0953-8984/23/29/296003

Atomistic magnetization dynamics in nanostructures based on first principles calculations: application to Co nanoislands on Cu(111)

D Böttcher[1,2], A Ernst[1] and J Henk[1]

[1] Max-Planck-Institut für Mikrostrukturphysik, Weinberg 2, D-06120 Halle (Saale), Germany
[2] Institut für Physik, Martin-Luther-Universität Halle-Wittenberg, D-06120 Halle (Saale), Germany

E-mail: dboettch@mpi-halle.de

Received 12 April 2011, in final form 9 June 2011
Published 30 June 2011
Online at stacks.iop.org/JPhysCM/23/296003

Abstract
The magnetization dynamics of Co nanoislands on Cu(111) is studied on the atomic scale by means of the stochastic Landau–Lifshitz–Gilbert equation. The exchange and anisotropy constants of the spin Hamiltonian are computed from first principles. We focus on hysteresis loops and magnetic switching in dependence on temperature, island size, and strength of an external magnetic field. The magnetic switching of nanoislands whose magnetization is reversed on the sub-nanosecond time scale is found consistent with the Stoner–Wohlfarth theory. We separate the superparamagnetic from the ferromagnetic regime and provide evidence that nanodomains can exist at least on a sub-picosecond time scale.

(Some figures in this article are in colour only in the electronic version)

1. Motivation

Over the years, the sizes of magnetic devices (e.g. sensors and spin electronic devices) have been strongly reduced. As a consequence, the dynamics of the devices' magnetization becomes increasingly important. Especially for magnetic recording and switching, the stability of the magnetization against thermal fluctuations is essential. On one hand, the size-dependent Curie temperature [1, 2] sets a lower limit for the device's extension. On the other hand, external parameters, such as the temperature and an external magnetic field, determine the dynamics as well.

The magnetization dynamics on the micro- and nanometer length scales is successfully described by micromagnetic simulations [3–5]. In these calculations, the local magnetization can be viewed as an average over tens or even hundreds of atomic magnetic moments. Because details of the magnetization dynamics on an atomic scale are lost, this approach is not well suited for studies of small systems of up to, say, a few hundred atoms.

With respect to the former, there is a need for theoretical magnetization dynamics investigations of small systems that rely on first principles calculations of the electronic and magnetic properties, complementing micromagnetic simulations. In this paper we report on such a study of Co nanoislands on Cu(111), following the approach of Skubic *et al* [6]. For the magnetization dynamics on the atomic scale, a local magnetic moment is attached to each site (atom). Therefore, an obvious basis of the approach is the classical Heisenberg model whose site-dependent exchange and magnetocrystalline anisotropy constants are obtained from first principles calculations. The dynamics of the local magnetic moments is described by the stochastic Landau–Lifshitz–Gilbert equation, with the Gilbert damping α being the only adjustable parameter [7–9].

Co nanoislands on Cu(111) themselves lend support to an investigation because they can be well controlled in experiments. The magnetic switching in these islands has been investigated by Rodary *et al* [10], using a low-temperature scanning tunneling microscope with an external magnetic

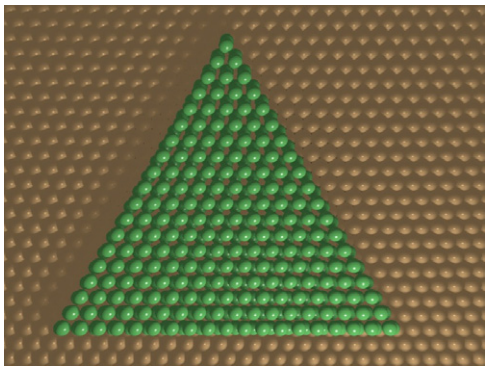

Figure 1. Artist's view of a Co nanoisland with a thickness of 2 monolayers on Cu(111). Co atoms: green (dark gray) spheres; Cu atoms: red (light gray) spheres.

field perpendicular to the surface. Three regimes have been identified with respect to the island size. For small islands, the coercive field is zero, which is explained by superparamagnetic behavior. This regime is followed by a strong increase of the coercive field with island size. It is qualitatively explained by a single-domain state in the spirit of Stoner–Wohlfarth theory [11]. For even larger islands, the switching field decreases, which is attributed to multi-domain states.

With regard to the abovementioned experiments [10], we mainly address hysteresis loops and magnetic switching of islands with up to 400 atoms. The main questions to be answered comprise the quantities and parameters at which the reversal takes place: island size, temperature, and strength of an external magnetic field. Further, we investigate whether the Stoner–Wohlfarth macrospin model applies even for small islands. We also show rather short-lived magnetic nanodomains that can exist in principle.

This paper is organized as follows. In section 2 we present our theoretical approach for Co/Cu(111). Results are discussed in section 3 for magnetic nanodomains (section 3.1), hysteresis loops and magnetic switching (section 3.2), as well as magnetic stability (section 3.3). We conclude with an outlook in section 4.

2. Theory

2.1. Co islands on Cu(111)

Co nanoislands of 2 monolayer (ML) height show a triangular shape (figure 1; cf [12–15]). The Co atoms follow the fcc(111) parent lattice of the Cu substrate, but the islands' orientation depends on whether a stacking fault is present ('hcp') or not ('fcc') [16]. The orientation mainly has implications for the adatom kinetics and growth of the islands [17], rather than for the exchange interactions (see section 2.3).

2.2. Spin Hamiltonian

In the atomistic approach, local magnetic moments $\boldsymbol{m}_i$ are attached to each site i at $\boldsymbol{r}_i$ ($|\boldsymbol{m}_i| = 1$). The spin Hamiltonian

$$\hat{H} \equiv \hat{H}_{\mathrm{ex}} + \hat{H}_{\mathrm{mca}} + \hat{H}_{\mathrm{dip}} + \hat{H}_{\mathrm{ext}} \tag{1}$$

comprises the exchange interaction

$$\hat{H}_{\mathrm{ex}} = -\sum_{ij} J_{ij} \boldsymbol{m}_i \cdot \boldsymbol{m}_j \tag{2}$$

of the classical Heisenberg model and the uniaxial magnetocrystalline anisotropy

$$\hat{H}_{\mathrm{mca}} = \sum_i K_i \left(m_i^z\right)^2 \tag{3}$$

(z surface normal). The sets of exchange constants J_{ij} and anisotropy constants K_i were computed from first principles (section 2.3). The dipolar interaction

$$\hat{H}_{\mathrm{dip}} = -\sum_{ij} \boldsymbol{m}_i^{\mathrm{t}} \underline{\underline{Q}}_{ij} \boldsymbol{m}_j, \qquad i \neq j, \tag{4}$$

accounts for the shape anisotropy, with the elements of $\underline{\underline{Q}}_{ij}$ given by

$$Q_{ij}^{\mu\nu} = \frac{\mu_0}{8\pi} \frac{3 r_{ij}^{\mu} r_{ij}^{\nu} - r_{ij}^2 \delta^{\mu\nu}}{r_{ij}^5}, \qquad \mu, \nu = x, y, z,$$
$$r_{ij} \equiv |\boldsymbol{r}_i - \boldsymbol{r}_j|. \tag{5}$$

An external magnetic field $\boldsymbol{B}_{\mathrm{ext}} = B_{\mathrm{ext}} \boldsymbol{e}_z$ is applied along the surface normal, leading to the Zeeman term

$$\hat{H}_{\mathrm{ext}} = -\sum_i \boldsymbol{B}_{\mathrm{ext}} \cdot \boldsymbol{m}_i. \tag{6}$$

2.3. Exchange and anisotropy constants

Prior to the magnetization dynamics calculations, we computed the electronic and magnetic structure of 2 ML thick Co films on Cu(111) from first principles, using a multiple-scattering approach. Our scalar-relativistic and relativistic Korringa–Kohn–Rostoker methods [18] rely on the local spin-density approximation to density-functional theory and utilizes the Perdew–Wang exchange–correlation potential [19].

Based on these *ab initio* calculations, both the exchange constants J_{ij} and the anisotropy constants K_i have been computed for a laterally infinite 2 monolayer thick Co film on Cu(111), using the magnetic-force theorem [20–25]. Consequently, edge effects in the islands are neglected but the Cu substrate is fully taken into account.

We studied Co films in both fcc and hcp stacking and found minor differences in the local magnetic moments. Also, the Heisenberg exchange constants depend marginally on the stacking (relative difference less than 1.2%). Therefore, we consider only fcc islands in this paper.

The exchange constants J_{ij} decay rapidly with distance r_{ij} between the sites i and j (figure 2). The J_{ij} are positive for the first three shells, indicating ferromagnetic coupling, but change sign with increasing distance. Monte Carlo calculations give a Curie temperature of 1140 K, which corresponds nicely to a value of about $0.75 T_{\mathrm{C}}$ (bulk) $\approx$ 1041 K, as estimated by Díaz-Ortiz *et al* [26] (T_{C} (bulk) = 1388 K [27]).

Compared to the local magnetic moments of Co (top layer: 1.70 μ_{B}; subsurface layer: 1.66 μ_{B}), the magnetic moments in the Cu substrate are negligibly small (less than

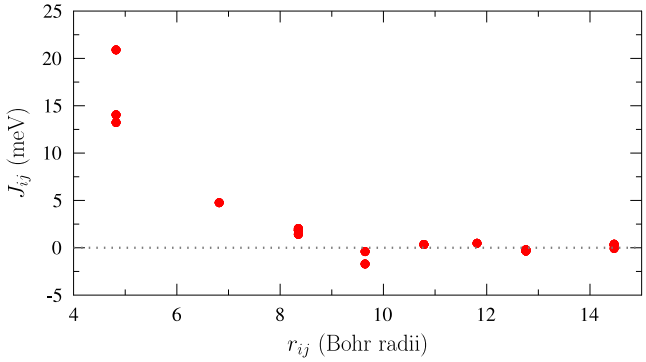

Figure 2. Heisenberg exchange constants J_{ij} of a 2 monolayer thick Co film on Cu(111) versus distance $r_{ij} \equiv |\boldsymbol{r}_i - \boldsymbol{r}_j|$ of Co sites i and j.

0.01 μ_B). Consequently, the exchange constants of Co–Cu pairs are three orders of magnitude smaller than those between nearest-neighbor Co pairs ($|J| < 0.02$ meV for Co–Cu, but $|J| \leqslant 20.9$ meV for Co–Co). Hence, we can safely restrict ourselves to the exchange interaction between Co atoms and neglect those between Co and Cu atoms in (2).

The layer-dependent anisotropy constants K_i are negative, indicating perpendicular anisotropy (top layer: -0.059 meV; subsurface layer: -0.011 meV) in agreement with experiment (Farle *et al* give -0.040 meV/atom at room temperature [28]) and theory [29].

2.4. Atomistic magnetization dynamics

The magnetization dynamics of the Co islands is described by the stochastic Landau–Lifshitz–Gilbert equation

$$\frac{\partial \boldsymbol{m}_i}{\partial t} = -\gamma \boldsymbol{m}_i \times \boldsymbol{B}_i + \frac{\alpha}{m} \boldsymbol{m}_i \times \frac{\partial \boldsymbol{m}_i}{\partial t}, \qquad (7)$$

with the gyromagnetic ratio γ and the Gilbert damping $\alpha \ll 1$. The two terms account for precession and relaxation with respect to the local effective field

$$\boldsymbol{B}_i = -\frac{\partial \hat{H}}{\partial \boldsymbol{m}_i} + \boldsymbol{b}_i(t). \qquad (8)$$

Here, the local temperature-dependent random fields $\boldsymbol{b}_i(t)$ account for thermal fluctuations [6, 30]. Following Langevin dynamics these fulfil

$$\langle b_i^\mu(t) \rangle = 0, \qquad \langle b_i^\mu(t) b_j^\nu(t') \rangle = \sigma^2 \delta_{ij}^{\mu\nu}\, \delta(t - t'). \qquad (9)$$

Their probability distribution is given by a Gaussian with width $\sigma = \sqrt{2\alpha k_B T/\gamma m}$.

The present modeling of thermal fluctuations by random local magnetic fields $\boldsymbol{b}_i(t)$ is in analogy to Brownian motion in which random forces act on the particles. The probability distribution of the fluctuations follows from the Fokker–Planck equation and the Langevin dynamics in which the Boltzmann distribution has to be recovered in thermal equilibrium. Since a detailed derivation is rather involved, we refer to publications of Skubic *et al* [6, 30].

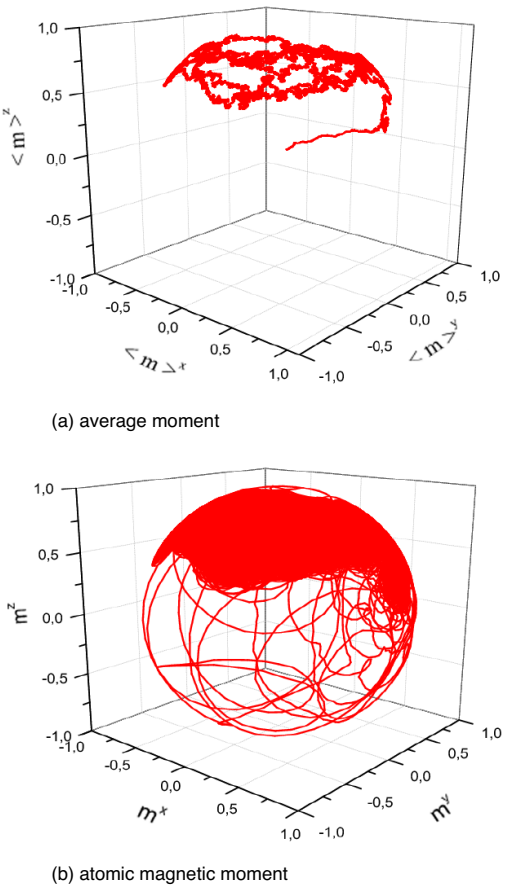

Figure 3. Magnetization dynamics in a Co island which is prepared in a random state. (a) Trajectory of the average magnetization $\langle \boldsymbol{m}(t) \rangle$, showing the precession around and the relaxation toward the easy axis (z axis). (b) Same as (a) but for a selected local moment $\boldsymbol{m}_i(t)$. Total duration 0.3 ns, temperature $T = 8$ K, island size $N_{\mathrm{isl}} = 36$ atoms.

We now briefly discuss the effect of thermal fluctuations. The average magnetization $\langle \boldsymbol{m}(t) \rangle$ of an island precesses counterclockwise around and relaxes slowly toward the easy axis (z axis; figure 3(a)). Thermal fluctuations appear as small deviations from the otherwise smooth trajectory. A selected $\boldsymbol{m}_i$ follows in general the trajectory of $\langle \boldsymbol{m}(t) \rangle$ but the deviations are much stronger (figure 3(b)), as is apparent from the broad circular 'band' in which the trajectory cannot be resolved in this representation.

By modeling thermal fluctuations as random local magnetic fields that act on the local magnetic moments, Stoner excitations are unlikely at the low temperatures addressed in this work. However, low-energy excitations (magnons) can show up, as has been investigated by the dynamical spin correlation function (not discussed here). In another approach to magnetization noise, introduced by Safonov and Bertram [31], mainly the low-energy eigenmodes are excited at low temperatures, a result which is consistent with the present modeling.

The damping constant α accounts for inelastic processes [32] and is fixed to 0.04 in the present study. In principle, α depends on the temperature [33–35]. It mimics the

coupling of the local magnetic moments to quasi-particles that dissipate energy (e.g. phonons). Since the properties of these quasi-particles depend on the temperature, the coupling and consequently the damping also depend on the temperature. Further, Steiauf and Fähnle [36] showed that the damping depends on the orientation of the $\boldsymbol{m}_i$, due to the anisotropy of the Fermi surface. This implies for nanoislands that the damping matrix $\underline{\underline{\alpha}}_i$ of a rim atom could differ considerably from that of an interior atom, especially in very small systems.

For the analysis of the magnetization dynamics we utilize the spin–spin correlation function

$$S(d;t) \equiv \langle \boldsymbol{m}_i(t) \cdot \boldsymbol{m}_j(t) \rangle_{d=|\boldsymbol{r}_i - \boldsymbol{r}_j|} \tag{10}$$

which quantifies the mutual alignment of magnetic moments separated by a distance d. The average is over the entire island.

Concerning hysteresis loops, we changed the external magnetic field B_{ext} in finite steps. A maximum field of 2 T drives the magnetization into saturation. At each constant B_{ext}, the system evolves for a duration of 30 ps (rest time). The results presented in section 3.2 are robust against the size of the magnetic field steps and against changes of the rest time, provided the rest time is long enough to allow for relaxation to a collinear state.

In the present investigation we applied Monte Carlo simulations [37, 38] for searching for ground-state configurations and critical temperatures. For the magnetization dynamics calculations within the SLLG framework, the equation of motion (7) for the local magnetic moments is integrated in time; this provides the realistic (femtosecond) time scale. The SLLG equation was also used to deduce ground-state configurations.

3. Results and discussion

3.1. Magnetic nanodomains

As stated in section 1, it is *per se* not clear how the magnetization reversal in nanoislands takes place. On one hand, the islands' magnetization could reverse coherently, as in the Stoner–Wohlfarth theory. Or on the other hand, the reversal could proceed via the formation of nanodomains in which island corners could play a significant role due to the lower atomic coordination.

It is obvious that nanodomains cannot exist in such small islands in the long term. However, it is conceivable that they can show up on very short time scales, especially if the system is highly perturbed, e.g. by an abrupt change of an external magnetic field. Therefore, we have investigated—as a prerequisite of the following discussions—the evolution of a system which is prepared in a random configuration; such a high-energy configuration allows us to determine the essential minimum rest time used for the hysteresis-loop calculations (section 3.2).

The evolution toward a ferromagnetic (collinear) state is studied by means of the correlation function $S(d;t)$ for $B_{\mathrm{ext}} = 0$. At $t = 0$, the small absolute values of $S(d;t)$ at distances $d > 0$ indicate a random state with small magnetization (white in figure 4). With time marching on, the local moments in the close vicinity of a local moment become parallelly aligned ($S(d,t) > 0$ for small d; area in red or dark gray with $+$). This area increases almost linearly with t.

At $t \approx 100$ fs, the collinearly aligned region around a local moment extends up to $d \approx 30$ bohr radii. This area is followed by a region (from about 30 bohr radii to about 70 bohr radii) in which the moments are almost oppositely aligned ($S(d,t) < 0$; blue (gray with $-$) in figure 4). For even larger distances ($d > 70$ bohr radii), the moments become again parallelly aligned. Further, the extended regions with parallel (red or gray with $+$) and anti-parallel (blue or gray with $-$) alignment evidence that even in such small islands, with $N_{\mathrm{isl}} = 400$ Co sites, magnetic nanodomains show up, at least on a sub-picosecond time scale.

Snapshots of the islands' magnetic structures are obtained from the projection

$$s_i(t) \equiv \boldsymbol{m}_i(t) \cdot \frac{\langle \boldsymbol{m}(t) \rangle}{|\langle \boldsymbol{m}(t) \rangle|}. \tag{11}$$

Nanodomains would appear as separated by abrupt changes (with a wall width of a very few lattice constants), whereas a spin wave would show up as a gradual deviation from the average magnetization in an $s_i(t)$ map.

In the random initial configuration ($t = 0$ fs in figure 5), $s_i(t)$ reflects the local moments' orientations of individual sites. With increasing time, the regions with positive s_i increase in size and coalesce. At $t = 152$ fs, for example, there exist mainly two nanodomains: a large one and a significantly smaller one at the right edge of the island. The latter domain remains stable but changes position. More precisely, it moves to the top corner at $t = 300$ fs, moves back ($t = 402$ fs) and shrinks until it vanishes completely, leaving behind a ferromagnetic island. The islands become completely collinear after about 1.5–2.0 ps (not shown).

The magnetic structure of the individual layers (left and right columns in figure 5) is not correlated at small times, which is attributed to strong fluctuations. At later times (say $t \geqslant 150$ fs), the domain structure shows up in both layers.

From the study of several samples we conclude that island edges act as nucleation centers for magnetic nanodomains. In some cases, two corners served as nucleation centers (not shown here). The 'trapped domains' are rather persistent, which one may attribute to the small coordination number of the Co corner sites, as compared to those in the islands' centers.

Magnetic frustrations typically show up in triangular lattices with antiferromagnetic coupling, for example at an fcc(111) surface with negative effective Heisenberg exchange ($J < 0$). Also the interplay of magnetic anisotropy and dipolar coupling can lead to magnetic frustration, even in the case of vanishing exchange, as was shown for one dimensional chains by Serantes *et al* [39]. Hence, one might conclude that the appearance of transient nanodomains is due to magnetic frustrations. However, in Co/Cu(111), the Heisenberg exchange is the dominant contribution in the Hamiltonian and clearly prefers ferromagnetic ordering; this rules out magnetic frustrations as the origin of transient nanodomains.

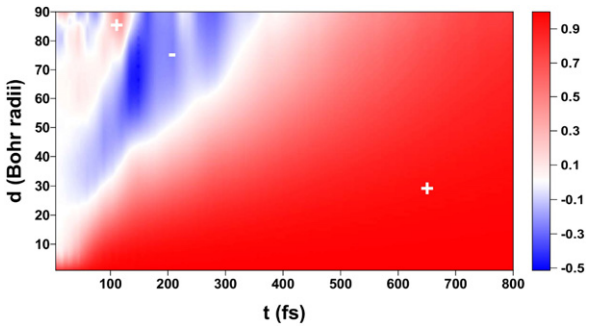

Figure 4. Spin correlation in a Co island. The spin–spin correlation function $S(d;t)$ is shown as color scale (gray scale) versus time t and distance d. At $t = 0$, the system is prepared in a random state which evolves into a ferromagnetic (collinear) state. After about 450 fs the island is completely collinearly magnetized, as is indicated by the red color (dark gray with + sign; + and − signs indicate the sign of $S(d,t)$). Temperature $T = 10$ K, island size $N_{\mathrm{isl}} = 400$ atoms.

3.2. Hysteresis loops and magnetic switching

We now turn to the magnetic switching upon application of an external magnetic field, with respect to scanning tunneling microscopy experiments by Rodary *et al* [10].

Ferromagnetic and superparamagnetic hysteresis loops are distinguished by the 'area' which is enclosed by the hysteresis curve: finite in the ferromagnetic regime but zero in the superparamagnetic regime. However, in the transition regime, the magnetization fluctuations are large and, consequently, the area does not allow the two regimes to separate clearly. Also the coercive field, as an alternative measure, fails in the determination of the transition temperature.

It turns out that better measures are $\langle\langle m(B_{\mathrm{ext}})\rangle\rangle$ averaged over the part of the hysteresis curve in which $B_{\mathrm{ext}} \leqslant 0$ T and $B_{\mathrm{ext}} \geqslant 0$ T,

$$\kappa_< \equiv \frac{1}{\mathrm{T}} \int_{B_{\mathrm{ext}} \leqslant 0} \langle\langle m(B_{\mathrm{ext}})\rangle\rangle \, \mathrm{d}B_{\mathrm{ext}} \qquad (12)$$

(B_{ext} in units of Tesla; the prefactor of 1/T(esla) makes $\kappa_<$ dimensionless) and similarly for $\kappa_>$. The 'double' average indicates the average of $\langle \boldsymbol{m}(t)\rangle$ over the duration τ in which B_{ext} is kept constant (section 2.4).

The general trend of $\kappa_>$ with temperature is understood as follows, for the example of an island with 36 atoms (figure 6). At low temperatures (inset for $T = 10$ K), the system is ferromagnetic, the coercive field is sizable (about 0.95 T), and the hysteresis loop is almost rectangular. Consequently, the top and the bottom parts of the hysteresis loop cancel partly in (12), making $\kappa_>$ small. With increasing temperature (inset for $T = 15$ K), the coercive field decreases (about 0.25 T), resulting in a reduced cancelation and an increased $\kappa_>$. At even higher temperatures (inset for $T = 20$ K), thermal fluctuations become pronounced, thereby reducing the cancelation further and still increasing $\kappa_>$. For very high temperatures (inset for $T = 100$ K), the thermal fluctuations are so strong that it is hardly possible to observe a hysteresis loop; hence, $\kappa_>$ decreases with temperature. An analogous consideration holds for $\kappa <$. We define the superparamagnetic–ferromagnetic transition temperature T_{trans} as the temperature

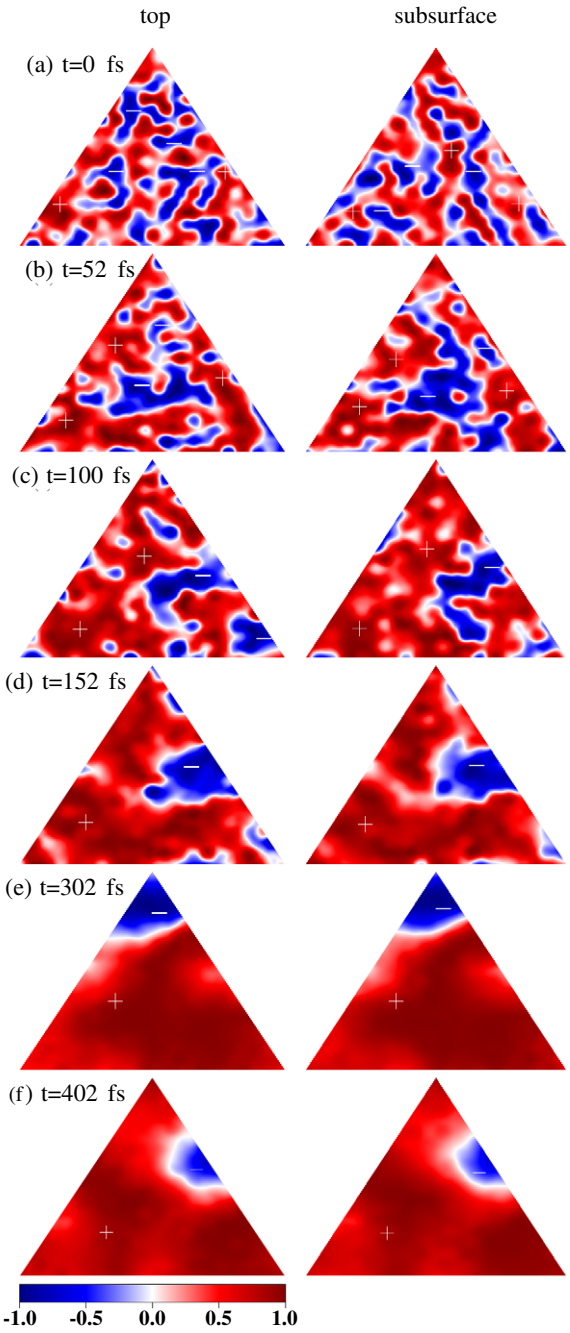

Figure 5. Temporal evolution of the magnetic structure in 2 ML-thick Co islands on Cu(111) which is prepared in a random state. The projection $s_i(t)$, defined in (11), is shown as color scale (gray scale) for the top Co layer (left column) and the subsurface Co layer (right column) at times $t = 0$, 52, 100, 152, 300, and 400 fs (from top to bottom). For clarity, $s_i(t)$ is interpolated between sites. The island edges are 91.6 bohr radii long, which corresponds to 20 atoms. $N_{\mathrm{isl}} = 400$ atoms, $T = 10$ K.

for which $\kappa_>$ is maximum and $\kappa_<$ is minimum, that is at 20 K for $N_{\mathrm{isl}} = 36$ atoms.

The transition temperature depends almost linearly on the island size, as is seen by the linear fit to the data in figure 7. The Curie temperature sets an upper limit for this temperature because the system will be paramagnetic at even

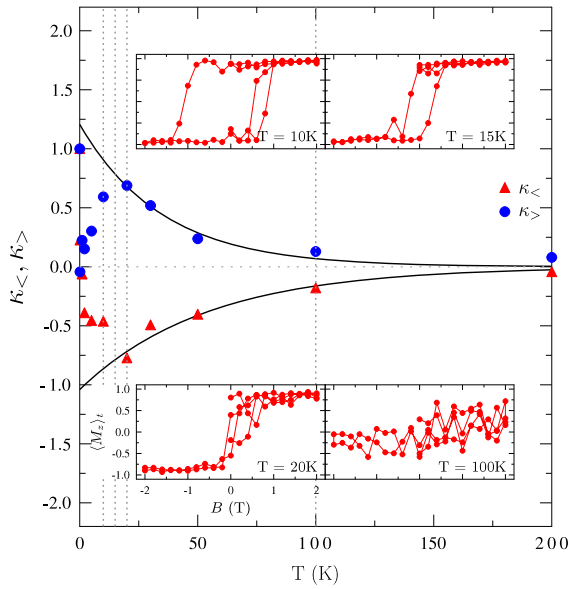

Figure 6. Transition from the superparamagnetic to the ferromagnetic state of a Co island on Cu(111). $\kappa_>$ and $\kappa_<$ (cf (12)) are displayed as symbols versus temperature T for an island of $N_{\rm isl} = 36$ atoms. Dotted vertical lines mark selected temperatures for which hysteresis loops are shown as insets. Both $\kappa_>$ and $\kappa_<$ show pronounced extrema at 20 K and decay in absolute value at higher temperatures. The lines present exponential fits $\kappa_> = \exp(aT + b)$ and $\kappa_< = -\exp(cT + d)$ to the data in the high-temperature regime ($\kappa_>$: $a = -0.02$ K^{-1} and $b = 0.04$; $\kappa_<$: $c = -0.03$ K^{-1} and $d = 0.19$). The errors in $\kappa_>$ and $\kappa_<$, largest at the transition temperature (here 20 K), are less than 10%.

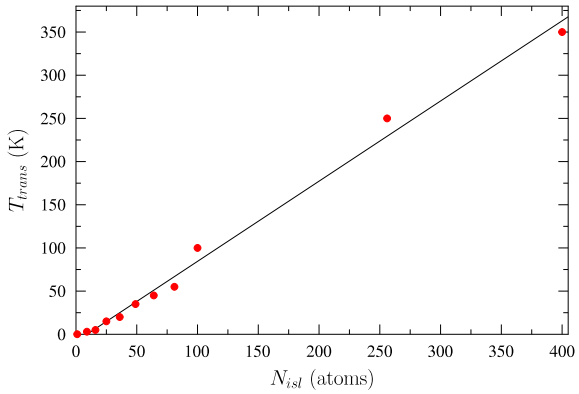

Figure 7. Transition temperature $T_{\rm trans}$ versus island size $N_{\rm isl}$ (symbols). The symbols represent averages over several samples (up to 10 samples per island size); the error is less than 10%. The line is a linear fit to the data, $T_{\rm trans} = aN_{\rm isl} + b$, with $a = 0.93$ K/atom and $b = -8.4$ K.

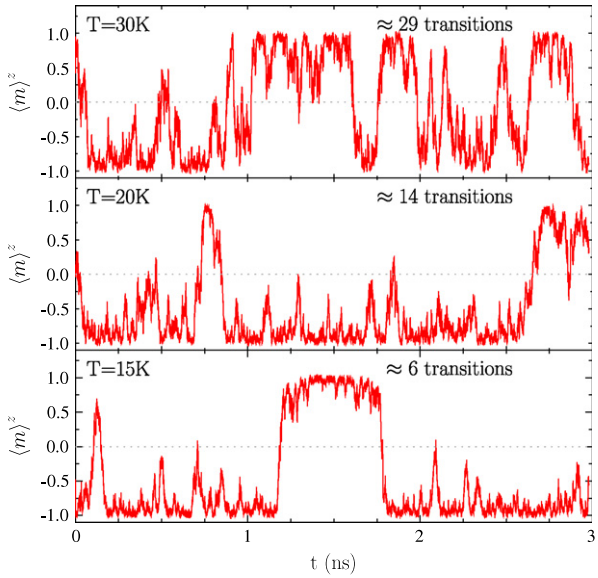

Figure 8. Temporal fluctuation of the magnetization in a Co island at different temperatures. The z-component $\langle m \rangle^z$ of the average magnetization is displayed versus time t for temperatures $T = 15$ K ((a), bottom), 20 K ((b), center), and 30 K ((c), top). In the period shown, $\langle m \rangle^z$ changes sign 6, 14, and 29 times (bottom to top). Island size $N_{\rm isl} = 36$ atoms, $B_{\rm ext} = 0$.

higher temperatures. This limit is reached for a roughly estimated island size of 1000 atoms.

By recording $S(d; t)$ during a complete hysteresis loop we show that Stoner–Wohlfarth theory is valid even for small islands on the time scale of today's experiments. Also for islands at the superparamagnetic–ferromagnetic transition (for example $T = 20$ K and $N_{\rm isl} = 36$ atoms in figure 6), thermal fluctuations play a marginal role: The local magnetic moments are almost collinear during the entire sweep. To be more precise, $S(d; t)$ and $s_i(t)$ range from 0.96 to 1.00 for all distances d and times t, indicating a collinear state without nanodomains.

Superparamagnetic and ferromagnetic states have been theoretically investigated by Shek *et al* [40]. The major difference from the present work is that Shek *et al* utilize Monte Carlo calculations which give a fictitious dynamics, whereas Landau–Lifshitz–Gilbert calculations provide a realistic dynamics on the femtosecond time scale. Further, the Heisenberg exchange constants were not calculated from first principles, in contrast to the present study.

3.3. Magnetic stability of Co nanoislands

In the Stoner–Wohlfarth theory, the stability of a magnetic system is related to the uniaxial magnetic anisotropy which produces a double-well potential for the macrospin of the system. A system is considered stable if the macrospin resides in one of the potential minima for a duration τ, which is assumed to be of the order of seconds [27]. Thermal fluctuations increase the rate of transitions from one minimum to the other and result in a superparamagnetic state, in dependence on temperature and island size.

We recorded the average magnetization of a 36-atom island for $B_{\rm ext} = 0$ at selected temperatures (figure 8). Since the uniaxial magnetocrystalline anisotropy prefers perpendicular anisotropy, we estimate roughly the magnetic stability by how often $\langle m(t) \rangle^z$ changes sign during recording (duration 3 ns, which is much smaller than the duration τ in the Stoner–Wohlfarth stability criterion). For temperatures of 15 K, 20 K, and 30 K—that is below, at, and above $T_{\rm trans}$ (figure 7)—we find 6, 14, and 29 flips, respectively. In other words, the islands are stable within about 0.5, 0.2, and 0.1 ns

on average, which provides upper limits for the time resolution necessary in experiments [10].

The above result can be related to the Stoner–Wohlfarth theory. The average time τ between switchings is proportional to $\exp(E/k_{\mathrm{B}}T)$, with the energy density $E = K\langle m_z\rangle^2$. We estimate the magnetic anisotropy density K to be 0.035 meV/atom, using the first principles results (section 2.3). This results for a 36-atom island in ratios of the average rest times of 1.6:1.3:1.0 for temperatures 15 K:20 K:30 K, whereas the *ab initio* ratios read 5:2:1. This means that the islands described by the stochastic Landau–Lifshitz–Gilbert equation flip less often than in Stoner–Wohlfarth theory, which we explain as follows. The Stoner–Wohlfarth macrospin can be viewed as rigidly 'glued' atomic magnetic moments; hence, temperature fluctuations act on all moments simultaneously and in the same manner. In contrast, the atomistic approach includes all (transverse) degrees of freedom of the individual atomic moments, and the temperature fluctuations act on each moment differently. Therefore, it is more unlikely that the magnetization of the entire island switches than in the Stoner–Wohlfarth model.

4. Concluding remarks

The stochastic Landau–Lifshitz–Gilbert equation in conjunction with the Heisenberg model is a powerful tool for detailed investigations of the magnetization dynamics of nanostructures, complementing micromagnetic simulations. Using first principles exchange and anisotropy constants, the calculations are based on state-of-the-art electronic and magnetic structure computations.

Even for small Co nanoislands on Cu(111) we showed that the magnetization switching is consistent with the Stoner–Wohlfarth theory, although nanodomains can in principle exist on a sub-picosecond time scale. By a detailed analysis of hysteresis loops in dependence on temperature, island size, and external magnetic field, we were able separate superparamagnetic and ferromagnetic regimes. Concerning the magnetic stability, the mismatch with scanning tunneling microscopy experiments [10] calls for improvements of the approach.

The present model can be amended by taking into account the site dependence of the exchange constants J_{ij} and of the anisotropy constants K_i. In particular, for very small islands, with a small number of atoms, these could be important. For example, the J_{ij} at the islands' edges could result in a noncollinear (canted) ground state which may affect the magnetic stability and the collinear–noncollinear transition.

Also the treatment of the damping allows for sophistication. The damping constant α, taken as constant in this work, depends on the temperature [35] and varies with the orientation of the local magnetic moments [36]. Although the spin–orbit coupling in Co is weak [41], the Dzyaloshinskii–Moriya interaction could be a further essential improvement of the theory [42]. Eventually, we note that with respect to low-temperature scanning tunneling microscopy experiments the model can be extended to current-induced effects, in the spirit of the *sd* model [43].

Acknowledgments

DB is a member of the International Max Planck Research School for Science and Technology of Nanostructures (nano-IMPRS, Halle/Saale, Germany). We gratefully acknowledge fruitful discussions with C Etz, G Rodary, D Sander, and S Wedekind. This work is supported by the *Sonderforschungsbereich* 762 'Functionality of Oxide Interfaces'.

References

[1] Pajda M, Kudrnovský J, Turek I, Drchal V and Bruno P 2000 Oscillatory Curie temperature of two-dimensional ferromagnets *Phys. Rev. Lett.* **85** 5424
[2] Kudrnovský J, Drchal V, Turek I, Pajda M and Bruno P 2002 Exchange interactions and Curie temperatures of 3D- and 2D-ferromagnets *Czech. J. Phys.* **52** 215
[3] Brown W F 1978 *Micromagnetics* (Huntington: Robert E Krieger Publishing)
[4] Miltat J, Albuquerque G and Thiaville A 2002 An introduction to micromagnetics in the dynamic regime *Spin Dynamics in Confined Magnetic Structures* (*Topics in Applied Physics*) ed B Hillebrands and K Ounadjela (Berlin: Springer) chapter 1, p 1
[5] Kronmüller H and Fähnle M 2003 *Micromagnetism and the Microstructure of Ferromagnetic Solids* (Cambridge, MA: Cambridge University Press)
[6] Skubic B, Hellsvik J, Nordström L and Eriksson O 2008 A method for atomistic spin dynamics simulations: implementation and examples *J. Phys.: Condens. Matter* **20** 315203
[7] Berger L 2001 Theory of Gilbert damping and ferromagnetic resonance linewidth in magnetic multilayers *J. Appl. Phys.* **90** 4632
[8] Šimánek E and Heinrich B 2003 Gilbert damping in magnetic multilayers *Phys. Rev.* B **67** 144418
[9] Capelle K and Gyorffy B L 2003 Exploring dynamical magnetism with time-dependent density-functional theory: from spin fluctuations to Gilbert damping *Europhys. Lett.* **61** 354
[10] Rodary G, Wedekind S, Sander D and Kirschner J 2008 Magnetic hysteresis loop of single Co nano-islands *Japan. J. Appl. Phys.* **47** 9013
[11] Stoner E C and Wohlfarth E P 1948 A mechanism of magnetic hysteresis in heterogeneous alloys *Phil. Trans. R. Soc.* A **240** 599
[12] Pietzsch O, Kubetzka A, Bode M and Wiesendanger R 2004 Spin-polarized scanning tunneling spectroscopy of nanoscale cobalt islands on Cu(111) *Phys. Rev. Lett.* **92** 057202
[13] Pietzsch O, Okatov S, Kubetzka A, Bode M, Heinze S, Lichtenstein A and Wiesendanger R 2006 Spin-resolved electronic structure of nanoscale cobalt islands on Cu(111) *Phys. Rev. Lett.* **96** 237203
[14] Niebergall L, Stepanyuk V S, Berakdar J and Bruno P 2006 Controlling the spin polarization of nanostructures on magnetic substrates *Phys. Rev. Lett.* **96** 127204
[15] Oka H, Ignatiev P A, Wedekind S, Rodary G, Niebergall L, Stepanyuk V S, Sander D and Kirschner J 2010 Spin-dependent quantum interference within a single magnetic nanostructure *Science* **327** 843
[16] Vázquez de Parga A L, García-Vidal F J and Miranda R 2000 Detecting electronic states at stacking faults in magnetic thin films by tunneling spectroscopy *Phys. Rev. Lett.* **85** 4365–8
[17] Negulyaev N N, Stepanyuk V S, Bruno P, Diekhöner L, Wahl P and Kern K 2008 Bilayer growth of nanoscale Co islands on Cu(111) *Phys. Rev.* B **77** 125437

[18] Zabloudil J, Hammerling R, Szunyogh L and Weinberger P (ed) 2005 *Electron Scattering in Solid Matter* (Berlin: Springer)
[19] Perdew J P and Wang Y 1992 Accurate and simple analytic representation of the electron–gas correlation energy *Phys. Rev.* B **45** 13 244
[20] Liechtenstein A I, Katsnelson M I, Antropov V P and Gubanov V A 1987 Local spin density functional approach to the theory of exchange interactions in ferromagnetic metals and alloys *J. Magn. Magn. Mater.* **67** 65
[21] Strange P, Ebert H, Staunton J B and Gyorffy B L 1989 A first principles theory of magnetocrystalline anisotropy in metals *J. Phys.: Condens. Matter* **1** 3947
[22] Daalderop G H O, Kelly P J and Schuurmans M F H 1990 First-principles calculation of the magnetocrystalline anisotropy energy of iron, cobalt, and nickel *Phys. Rev.* B **41** 11 919
[23] Wang X, Wang D-S, Wu R and Freeman A J 1996 Validity of the force theorem for magnetocrystalline anisotropy *J. Magn. Magn. Mater.* **159** 337
[24] Stiles M D, Halilov S V, Hyman R A and Zangwill A 2001 Spin-other-orbit interaction and magnetocrystalline anisotropy *Phys. Rev.* B **64** 104430
[25] Dhesi S S, van der Laan G, Dudzik E and Shick A B 2001 Anisotropic spin–orbit coupling and magnetocrystalline anisotropy in vicinal Co films *Phys. Rev. Lett.* **87** 067201
[26] Díaz-Ortiz A, Aguilera-Granja F and Morán-López J L 1996 Equilibrium thermodynamics of cobalt–copper slabs *Phys. Rev.* B **53** 6514
[27] Getzlaff M 2008 *Fundamentals of Magnetism* (Berlin: Springer)
[28] Farle M, Platow W, Kosubek E and Baberschke K 1999 Magnetic anisotropy of Co/Cu(111) ultrathin films *Surf. Sci.* **439** 146
[29] Hammerling R, Uiberacker C, Zabloudil J, Weinberger P, Szunyogh L and Kirschner J 2002 Magnetic anisotropy of thin films of Co on Cu(111) *Phys. Rev.* B **66** 052402
[30] Skubic B 2007 Spin Dynamics and Magnetic Multilayers *PhD Thesis* Uppsala Universitet, Uppsala
[31] Safonov V L and Bertram H N 2002 Nonuniform thermal magnetization noise in thin films: application to GMR heads *J. Appl. Phys.* **91** 7279
[32] Hickey M C and Moodera J S 2009 Origin of intrinsic Gilbert damping *Phys. Rev. Lett.* **102** 137601
[33] Gilmore K, Idzerda Y U and Stiles M D 2007 Identification of the dominant precession-damping mechanism in Fe, Co, and Ni by first-principles calculations *Phys. Rev. Lett.* **99** 027204
[34] Starikov A A, Kelly P J, Brataas A, Tserkovnyak Y and Bauer G E W 2010 A unified first-principles study of Gilbert damping, spin-flip diffusion, and resistivity in transition metal alloys *Phys. Rev. Lett.* **105** 236601
[35] Ebert H, Mankovsly S, Ködderitzsch D and Kelly P J 2011 *Ab initio* calculation of the Gilbert damping parameter via linear response formalism, arXiv:1102.4551v1 [cond-mat.mtrl-sci]
[36] Steiauf D and Fähnle M 2005 Damping of spin dynamics in nanostructures: an *ab initio* study *Phys. Rev.* B **72** 064450
[37] Binder K and Heermann D W 1997 *Monte Carlo Simulation in Statistical Physics: An Introduction* 3 edn (Berlin: Springer)
[38] Metropolis N, Rosenbluth A W, Rosenbluth M N and Teller E 1953 Equation of state calculations by fast computing machines *J. Chem. Phys.* **21** 1087
[39] Serantes D, Baldomir D, Pereiro M, Hernando B, Prida V M, Sánchez Llamazares J L, Zhukov A, Ilyn M and González J 2009 Magnetic ordering in arrays of one-dimensional nanoparticle chains *J. Phys. D: Appl. Phys.* **42** 215003
[40] Shek C H, Shao Y Z and Lai J K L 2000 Transition from superparamagnetism to ferromagnetic single-domain in a Heisenberg model for nano-cluster magnetic systems *Physica* **276** 201
[41] Pickel M, Schmidt A B, Giesen F, Braun J, Minár J, Ebert H, Donath M and Weinelt M 2008 Spin–orbit hybridization points in the face-centered-cubic cobalt band structure *Phys. Rev. Lett.* **101** 066402
[42] Udvardi L, Szunyogh L, Palotás K and Weinberger P 2003 First-principles relativistic study of spin waves in thin magnetic films *Phys. Rev.* B **68** 104436
[43] Zhang S and Li Z 2004 Roles of nonequilibrium conduction electrons on the magnetization dynamics of ferromagnets *Phys. Rev. Lett.* **93** 127204